To be published in the proceedings of the
First Symposium on Nuclear Physics in the Universe, Oak-Ridge TN, September 1992
(Adam Hilger & Co., Bristol U.K.) Ed. M. R. Strayer and M. W. Guidry.

The GEMINGA neutron star : Evidence for nucleon superfluidity at very high density

Dany Page

Department of Astronomy, Columbia University, 538 West 120th Street, New York, NY 10027

Abstract. A comparison of the recent age and temperature estimates of the Geminga neutron star with cooling models is presented. This star is already in the photon cooling era and it is shown that its temperature can be understood within both the slow and fast neutrino emission scenarios and consequently will not allow discrimination between these two scenarios. However in both cases agreement of the theoretical cooling curves with the observed temperature depends crucially on the presence of nucleon pairing in most, if not all, of the core.

1. Introduction

The study of the thermal evolution of young neutron stars offers the possibility to obtain unique information about the structure of compressed cold nuclear matter. The early cooling after the supernova explosion is driven by neutrinos whose emission rate is a very sensitive function of the state of that matter. Moreover, both the neutrino and the later photon coolings are strongly affected by the occurence of pairing (*à la* BCS) of the baryonic components in the star's core. These two effects give us two handles to extract information about nuclear matter through comparison with observed neutron stars of known age. The announcement of the definitive identification of Geminga as a spinning magnetized neutron star by Halpern & Holt this spring gave rise to great excitement in the astrophysical community. This object, which has been a mystery for many years [1], is suddenly revealing a wealth of informations thanks the ROSAT and GRO observatories. We present here a comparison of the Geminga observation with our latest cooling models and show what can be learned from it. These results will hopefully stimulate more detailed works on the various aspects of the models presented.

[1] *Geminga* stands for *Gemini Gamma-ray source*, but it also means 'does not exits' or 'is not there' in Milanese dialect [1].

2. Geminga

2.1. The story

Geminga was discovered in 1972 by the γ-ray telescope on SAS-2 [2] and was observed again five times by COS-B between 1975 and 1982. It was the second brightest source in the sky at energies above 100 MeV in the second COS-B catalog [3] where it was labelled 2CG195+04. Gamma-ray detectors did not have enough angular resolution to allow for search of an optical counterpart, but the situation changed when the EINSTEIN satellite could find four soft X-ray sources within the γ-ray error box. Analysis showed that only one of these sources, 1E0630+178, could be the counterpart of 2CG195+04 [1]. The angular resolution of EINSTEIN's HRI (90% confidence radius of 3") then allowed for optical search. 1E0630+178 points to a blank field on the Palomar Sky Survey plate but deeper observations revealed two stars in the error circle and the faintest one, with r-magnitude ~ 25.5, is presently considered as the optical counterpart of Geminga [4,5]. It thus took ten years to find Geminga in soft X-rays and more than fifteen years to identify it in the optical range. It has not yet been detected at radio wavelength.

Early on it was suspected that Geminga was an isolated neutron star but other models had been proposed. The situation dramatically changed this spring when Halpern & Holt [6] discovered pulsations at a period of 0.237 sec in their soft X-ray ROSAT observation of Geminga. Using this result, Bertsch *et al* [7] found the same period in the 1991 GRO γ-ray observation and Bignami & Caraveo [8] confirmed it in the archival COS-B data. This definitely identified 2CG195+04 and 1E0630+178 as the same object and proved unequivocally that Geminga is an isolated spinning magnetized neutron star.

2.2. The data

2.2.1. Geminga's age. The Geminga period as obtained in [6] is $P = 0.2370974\ s \pm 0.1\ \mu s$. The earlier observations by COS-B and later by GRO have slightly different P's which lie very accurately on straight line (see [8]) and give a practically constant period derivative $\dot{P} = 1.0977 \times 10^{-14}\ s\ s^{-1}$ [9] over a span of 16 years. From these we obtain its 'spin-down age' $\tau = \frac{1}{n-1} P/\dot{P} = 3.4 \times 10^5$ years with $n = 3$ (spin down index for magnetic dipole breaking). The relation between the spin-down age and the real age of a pulsar is a delicate problem, refer to [10,11,12] for discussions. We will take as extreme values the two case of $n = 2$ and $n = 4$, giving

$$2.3 \times 10^5 \text{yrs} \leq t \leq 6.8 \times 10^5 \text{yrs}, \tag{1}$$

the upper value being probably an overestimate.

2.2.2. Geminga's temperature. In the first estimate of the star temperature Halpern & Holt [6] fitted the two apparent components of the spectrum by a black body and a power law spectra. The best fit gave a blackbody temperature of $T = 3 - 4 \times 10^5$ K. In a second, more detailed, analysis Halpern and Ruderman [13] replace the power law component by a second black body with higher temperature and argue that this hotter component ($T \cong 3 \times 10^6$ K) is due to emission from a reheated polar cap (this temperature is too high to be explained only by anisotropic magnetic heat transport). They obtain for the main surface emission a temperature of $T = (5.2 \pm 1.0) \times 10^5$ K. From the ratio of the luminosities of these two components they conclude that the ratio of the areas of the hot and cold emitting regions is about 3×10^{-5}. Moreover it is likely that the surface is not emitting uniformly and that some colder region is not been seen, making the concept of 'surface temperature' an ambiguous one. However cooling calculations give as an output the effective temperature, i.e. a total luminosity, and the presence of a cooler region would reduce the luminosity and make the effective temperature somewhat lower than the above value of $(5.2 \pm 1.0) \times 10^5$ K.

All these analyses use black-body spectra but the surface of a neutron star cannot be expected to be a perfect black body. Romani [14], Miller [15] and Shibanov *et al* [16] have calculated more realistic spectra for various surface chemical compositions with ([15,16]) or without ([14]) magnetic field. The general trend of these results, for H, He or Fe atmospheres, is that there is an excess emission in the Wien tail of the spectrum compared to the blackbody which falls within the EINSTEIN and ROSAT detector ranges. This excess is reduced if metals are present (due to absorption edges) or when the effect of the magnetic field is taken into account. Use of these spectra will lower the measured temperature. Finally some contamination from a surrounding nebula and/or surface reheating by gamma-rays or particles from the magnetosphere cannot be excluded.

We will take for comparison with our calculations an effective temperature of $4 - 6 \times 10^5$ K ($= 10^{5.6-5.75}$ K) but insist that it has to be taken as an upper limit.

3. Neutron star cooling

After being formed hot in a supernova explosion, a neutron star cools by neutrino emission from its core and crust and by photon emission from its surface. Neutrino emissivities are proportional to T_i^8 or T_i^6, while photon emissivity is proportional to $T_s^4 \sim T_i^{2.2}$ (T_i is the interior temperature and T_s the surface temperature; $T_s \sim T_i^{0.55}$ [17]), consequently photons will eventually dominate when T_i has dropped sufficiently. The shift from neutrino to photon cooling usually occurs at about 10^5 years of age. Geminga is in the photon cooling era.

3.1. Neutrino processes

The dominant neutrino emission processes occur in the core of the star and are variant of beta and inverse beta decays. Table 1 shows the approximate relevant emissivities for comparison. One can divide them into slow and fast neutrino emission, depending if they involve four or two baryons. The difference between fast and slow emission comes mainly from phase space considerations, and the precise values depend on form factors, strangeness violation and strong interaction corrections. We refer to the recent review by Pethick [18] for a detailed discussion. There is still doubt about which processes can actually occur, but the number of proposed channels for fast cooling is now so large that it is becomming difficult to believe that none of these is permitted and that

Table 1. Some core neutrino emission processes and their emissivities. Hyperons, if present, can go into either modified or direct Urca processes with emissivities slightly lower than the corresponding purely nucleonic processes [19]. T_9 is the temperature in units of 10^9 kelvins.

Process Name	Process	Emissivity Q_ν (erg/sec/cm^3)
Modified URCA	$\begin{cases} n+n' \to n'+p+e^- + \overline{\nu_e} \\ n'+p+e^- \to n'+n+\nu_e \end{cases}$	$\sim 10^{20} \cdot T_9^8$ [20]
K-condensate	$\begin{cases} n+K^- \to n+e^- + \overline{\nu_e} \\ n+e^- \to n+K^- + \nu_e \end{cases}$	$\sim 10^{24} \cdot T_9^6$ [21]
π - condensate	$\begin{cases} n+\pi^- \to n+e^- + \overline{\nu_e} \\ n+e^- \to n+\pi^- + \nu_e \end{cases}$	$\sim 10^{26} \cdot T_9^6$ [22]
Direct URCA	$\begin{cases} n \to p+e^- + \overline{\nu_e} \\ p+e^- \to n+\nu_e \end{cases}$	$\sim 10^{27} \cdot T_9^6$ [23]
Quark URCA	$\begin{cases} d \to u+e^- + \overline{\nu_e} \\ u+e^- \to d+\nu_e \end{cases}$	$\sim 10^{26} \alpha_c T_9^6$ [24]

neutron star cooling follows the old 'standard model' with only the modified Urca process. Awaiting for a definite argument on this point we will still consider both the fast and slow cooling scenarios.

Deconfined quarks may be present in the center of massive neutron stars and are also copious neutrino emitters. They thus belong to the fast cooling scenario but obviously require a separate treatment. We will not consider them explicitely here.

3.2. Nucleon pairing

Pairing of nucleons in the neutron star core has a dramatic effect on the cooling, both by suppressing the neutrino emission and the specific heat. It was shown in [34] that the temperature at ages between $10^2 - 10^5$ years of a fast cooling neutron star is actually determined by the temperature T_c at which its core nucleons are paired. Since T_c is density dependent it is its lowest value (usually in the very center of the star) which is relevant. Theoretical calculations of T_c are extremelly difficult and the presently published values are still very uncertain. In the core, the protons are paired in the $^1S_0$ partial wave while the neutrons are in the $^3P_2$ partial wave. $^1S_0$ pairing is easier to study than $^3P_2$, but unfortunately, in the case of protons, it depends strongly on the relative concentrations of protons and neutrons since protons see mostly neutrons. For neutron $^3P_2$ pairing the proton fraction x_p is not so important as long as it is low, but the $^3P_2$ interaction is much more difficult to handle than the $^1S_0$ interaction (moreover the tensor interaction also introduces an important $^3F_2$ contribution).

Figure 1a shows the results of calculations of proton pairing critical temperatures.

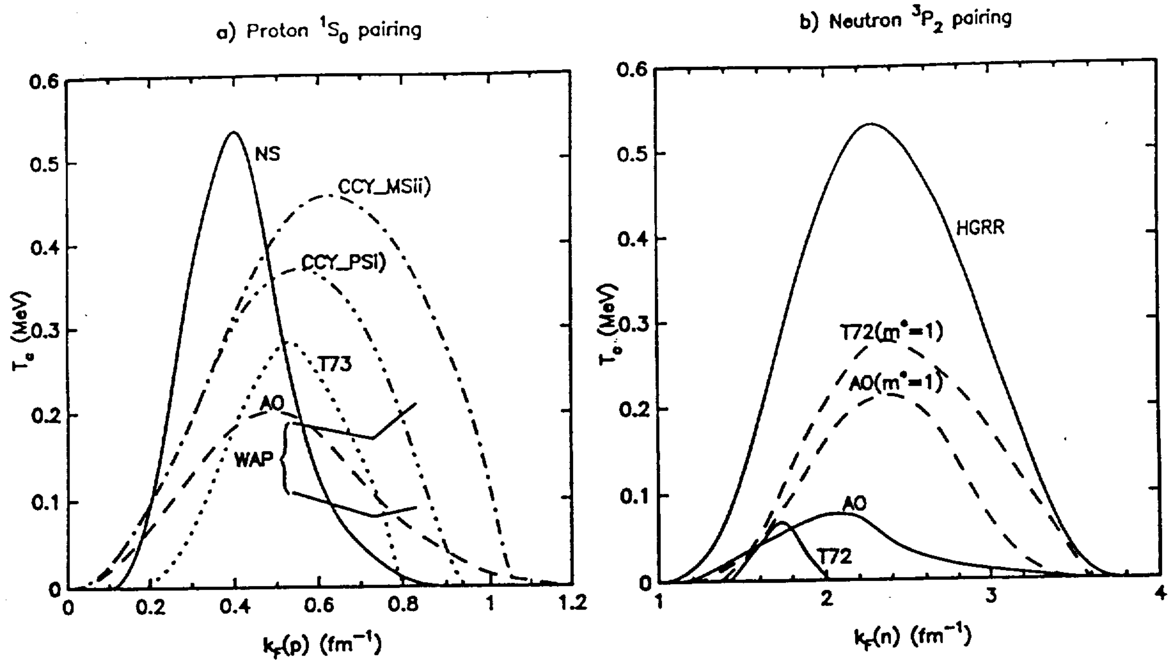

Figure 1. a) Proton $^1S_0$ pairing critical temperatures. CCY : [25], T73 : [26], NS : [27], AO : [28], WAP : [29].
b) Neutron $^3P_2$ pairing critical temperatures. HGRR : [30], T72 : [31], AO : [33]. The two dashed curves show the results of T72 and AO when the effective mass is fixed to the free mass value.

One sees that their maxima differ by a factor five and that there is also a large spread in the Fermi momentum at which T_c vanishes. The most recent calculation [29] is the first one to take properly into account the presence of the neutrons; it gives a lower T_c than the previous ones but which does not decrease with density as fast as in the previous calculations. However this results may change when a different proton fraction is used (T. Ainsworth, private communication).

Figure 1b shows the three calculations of neutron $^3P_2$ critical temperatures published to date. One sees that the maximum value of T_c as well as the Fermi momentum at which T_c vanishes differ enormously from one calculation to the other. The curves T72 [31] and AO [33] use the same nuclear potential but different many-body methods and give the same maximum T_c but very different vanishing densities. A fourth calculation [32] of the pairing interaction which includes medium effects not considered in the other ones seems to give a very high T_c and a strong dependence of the vanishing density on the potential. From this one sees that the value of T_c for neutron $^3P_2$ pairing and the density range where pairing occurs are still open questions.

If hyperons are present one can expect that they also pair for the same reasons as the nucleons do. With regard to quarks, pairing is also very probable [35].

The effect of pairing is to reduce the phase space available for excitations. As a result both the specific heat of the paired component and the neutrino processes to which it contributes will be suppressed. We treat this suppression by simply multi-

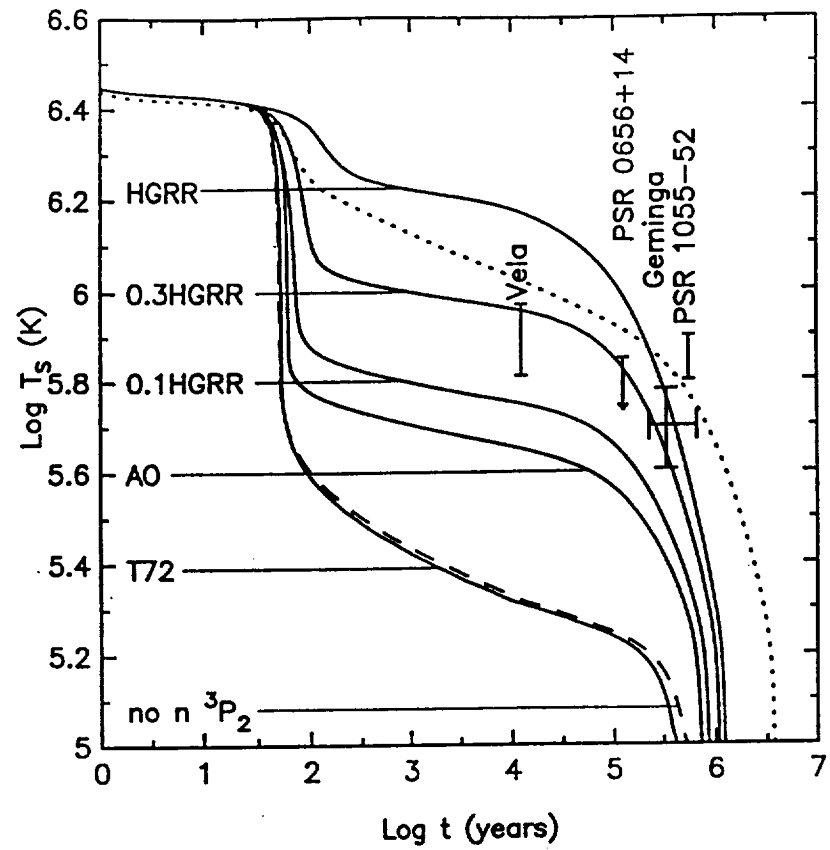

Figure 2. Cooling by the direct Urca process and neutron $^3P_2$ pairing suppression. The dashed curve show the cooling by direct Urca with no core pairing. All continuous curve have direct Urca and core neutron pairing with various T_c from Figure 1b); the 0.3HGRR and 0.1HGRR have pairing from HGRR with T_c multiplied by 0.3 and 0.1 respectively. The dotted curve show the cooling with only the modified Urca and no core pairing for comparison. In all cases the crust neutrons are paired with T_c from [36]. The cross shows the Geminga value, the other three data points are as in [34] (they should also be plotted with an uncertainty on the age).

plying the corresponding normal values by a Boltzmann factor $\exp(-\Delta/k_BT)$. This is correct when $T \ll T_c$ but overestimate the suppression near T_c since there the gap Δ vanishes. Accurate suppression factors are being calculated by Levenfish & Yakovlev and will be available soon for a more quantitative treatment.

4. Comparison with Geminga

4.1. Fast cooling scenario

In the fast cooling models one accepts early enhanced neutrino emission, by the direct URCA process or by some 'exotic' matter, but must then suppress the emission by

Table 2. Some properties of the EOS's used. Columns two to four list the mass, central density and central proton fraction of a maximum mass star. Columns five to seven give properties of a $1.4 M_\odot$ star : radius, central density and central proton fraction. (The PAL EOS's are labelled PALij, i,j=1,2,3, where i refers to the symmetry energy function and j to the compression modulus)

EOS	Maximum mass star			$1.4\ M_\odot$ star		
.	$M_{max}(M_\odot)$	$\rho_{max}(fm^{-3})$	$x_p(\%)$	$R(km)$	$\rho_c(fm^{-3})$	$x_p(\%)$
FP [38]	1.79	1.18	~ 0	10.85	0.69	2.0
WFF(av14) [39]	2.10	1.25	4.8	10.60	0.64	9.6
MPA [40]	2.44	0.89	19.0	12.45	0.41	9.0
PAL32 [41]	1.68	1.51	15.2	11.02	0.74	11.4
PAL33 [41]	1.90	1.24	14.0	11.91	0.54	9.7

nucleon superfluidity (Page & Baron [37] and Page & Applegate [34]). Without superfluidity suppression the resulting surface temperature is much below the estimated value for any neutron star observed so far. Figure 2 show typical cooling curves, from [34], with the direct Urca process and various $^3P_2$ neutron gaps. A large gap as calculated by Hoffberg *et al* [30] almost completely turn off the core emission while the small gap from Takatsuka [31] has almost no effect because most of the core remains normal. Intermediate values give reasonable agreement with the Geminga temperature. See [34] for more details.

The fast neutrino emission is so efficient that any region in the star which remains normal will drive the surface temperature well below the observed temperature of Geminga. Consequently within the fast cooling scenario one of the neutrino emitting components must be paired at the highest densities reached in the core. If hyperons are present the same conclusion holds since even a small amount of Λ will allow a direct Urca reaction [19]. If both Λ and Σ^- are present they participate into a purely hyperonic direct URCA process and thus one of them must be paired. One may expect hyperons to have a lower T_c if they have weaker interactions than nucleons and if this is the case what controls the cooling is the Λ or Σ^- pairing critical temperature.

4.2. Slow cooling scenario

While with the fast cooling scenario one needs pairing to reduce the cooling, within the slow cooling scenario one encounters the opposite problem : neutrino emission is not sufficient and one needs to speed up the cooling during the photon era by reducing the specific heat through nucleon pairing. This slow cooling scenario, often called the 'standard model', assumes that the only core neutrino emission is by the modified Urca process and the two (less efficient) similar processes with neutral currents. Comparison with the standard calculations of Nomoto and Tsuruta [42] (or

Table 3. Normal specific heat, at $T = 10^9$ K, of neutrons, protons and electrons in the core and crust of a $1.4M_\odot$ neutron star built with the five EOS's used. (Units are 10^{38} $ergs\ K^{-1}$, i.e. $C_v(T) = (\text{Table} - \text{Entry}) \times (T/10^9K) \times 10^{38}\ ergs\ K^{-1}$).

EOS	Core components			Crust components	
.	n	p	e	n	e
FP	9.00	2.89	0.50	0.97	0.025
WFF(av14)	9.31	2.81	0.51	0.72	0.018
MPA	11.9	3.90	0.67	1.60	0.044
PAL32	10.5	3.58	0.67	1.60	0.044
PAL33	9.66	3.41	0.68	1.16	0.031

similar resluts by Van Riper [43]) shows that some EOS's can produce a star with the observed temperature of Geminga, but other still give too high a temperature. However these authors do not consider the enormous uncertainty in the density at which the gap vanish : their 'successful' models are simply the ones with stiff EOS (i.e. low central density) which have hence pairing in the full core. To avoid this misleading interplay between the EOS stiffness and the density dependence of the gap we take density independent gaps, therefore forcing pairing in the full core. We consider five different EOS's from modern calculations, relativistic and non-relativistic, which encompass a large range of stiffness and proton fraction. Their properties are summarized in Table 2. We reject EOS's with proton fractions large enough to allow the direct Urca process in a $1.4M_\odot$ star, but do consider MPA, PAL32 and PAL33 which allow it only at higher masses. Table 3 shows the contribution to the specific heat of the various components in a 1.4 $M_\odot$ star at a temperature $T = 10^9K$ without pairing. Pairing will suppress C_v exponentially when $T \ll T_c$ and the corresponding specific heat will practically disappear. In all our calculations the crust neutrons are paired using the gap from [36] and their contribution to C_v is thus strongly reduced; the crust electrons have a negligible contribution as well as the crust lattice. One can see from the table that the core neutrons contribute about $\frac{3}{4}$ of the total specific heat, the protons $\frac{1}{4}$ and the core electrons about 0.5 %. These fractions are suprisingly almost independent of the EOS.

The cooling curves for 1.4 $M_\odot$ stars built with our five EOS's are compared in Figure 3 with the Geminga observation. When no core pairing occurs (a) the theoretical results are consistent only with the higher surface temperature T_s and the older age: taking into account that this T_s is certainly an overestimate and considering also that several reheating mechanisms [44,45] should raise the temperature of the theoretical curves at this age, one can state that Geminga's temperature is incompatible with these cooling models (unless Geminga's age is underestimated). With pairing of the protons (b) the discrepancy increases because of the suppression of the early neutrino

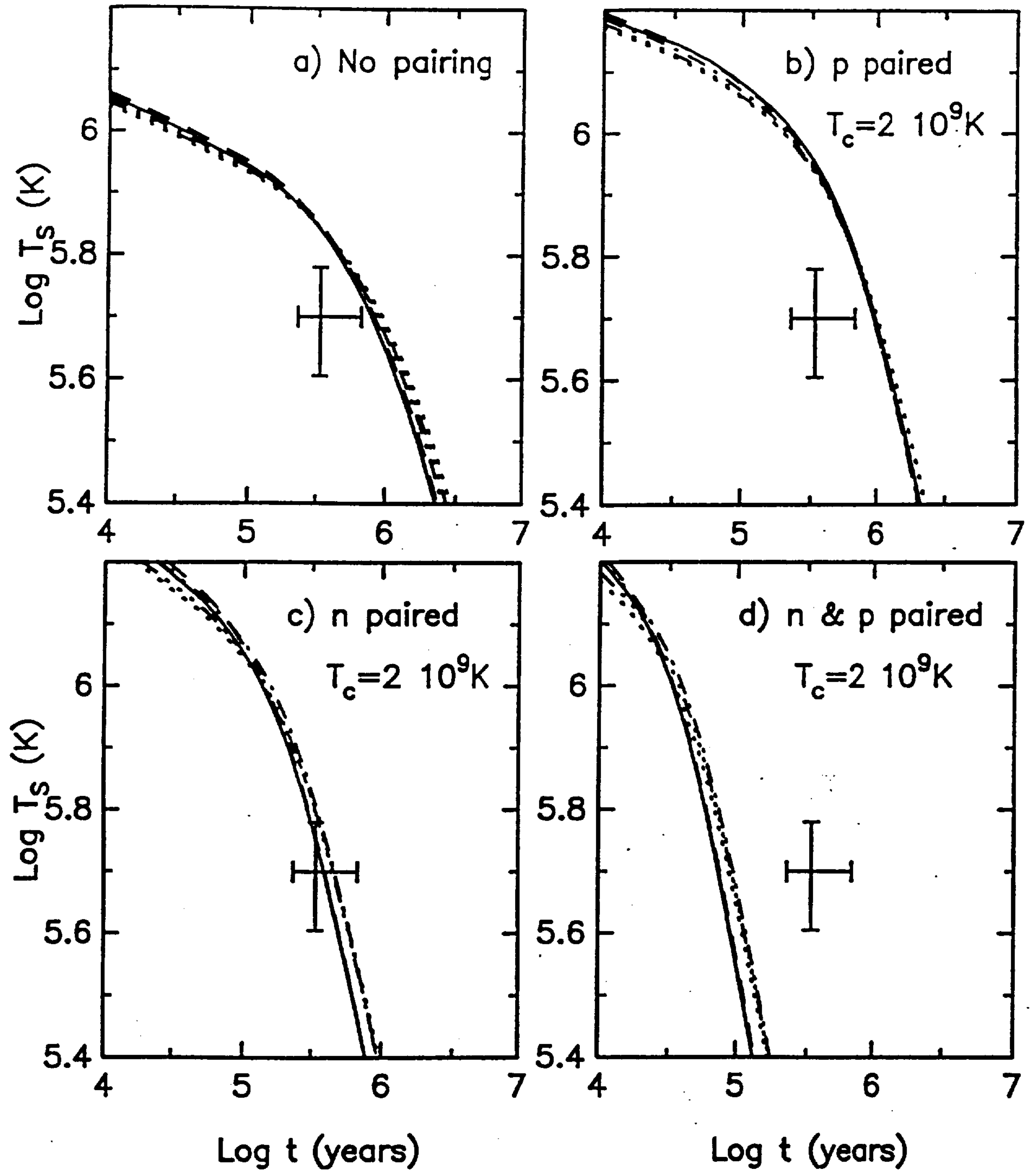

Figure 3. **Cooling by the modified Urca process without/with pairing(s) and five different EOS's : FP ——, WFF(av14) – – –, MPA · · · · ·PAL32 — · —and PAL33 — · · · —. In all cases the crust neutrons are paired with T_c from [29]. The cross shows the Geminga value.**

a) No core pairing at all.

b) Protons paired with density independent $T_c = 2 \times 10^9$ K.

c) Core neutrons paired with density independent $T_c = 2 \times 10^9$ K.

d) Protons and core neutrons paired with density independent $T_c = 2 \times 10^9$ K.

cooling and the only small ($\sim 25\%$) decrease of the specific heat in the photon cooling era. When neutrons are paired (c) the reduction of C_v is large enough to accomodate the observed temperature. If both neutrons and protons are paired (d) within the whole core C_v is cut down by a factor 20 (only the electron contribution is left) and the temperature drop in the photon cooling era is extremely fast; however reheating mechanisms could be very efficient here, due to the very low C_v, and rise the curve significantly. The curves for the various EOS's are very similar when identical T_c are used, showing that the EOS-dependent results obtained in other works (e.g. [42,43]) are mostly due to the density dependence of T_c that the authors choose. The only thing that one can say about the value of T_c is that it has to be high enough for the specific heat to be sufficiently suppressed, the value of 2×10^9 K used is only illustrative.

If one relieves the approximation of a density independent gap two things can happen. Close to the crust-core boundary where neutron pairing shifts from $^1S_0$ to $^3P_2$ there may be a thin layer where T_c is vanishingly small : this layer would contributes to C_v when the deeper parts are paired, but it comprises only a small shell. In the center of the star the density gradient is very small and a large mass is at density close to the maximum density : the neutron Fermi momentum is above 90 % of its center value in a region of mass larger than 0.3 $M_\odot$ for a 1.4 $M_\odot$ star from PAL33 and a mass larger than 0.6 $M_\odot$ with WFF(av14). Therefore if the central density is above the vanishing density for neutron pairing it cannot be much above it if we want a large enough reduction of C_v.

The envelope calculation used does not take into account the effect of the magnetic field on the heat transport. It has been argued that this effect is small [46] and hence our results should not change significantly when the magnetic field effects are included. A detailed analysis is in progress and will be published later.

5. Conclusion

We have compared the recent temperature measurement of the Geminga neutron star with cooling models and found that, since this star is old enough to be in the photon cooling era, both fast and slow neutrino emission mechanisms can explain it. One therefore cannot draw any conclusion about neutrino emission from dense nuclear matter using this observation only. However, a crucial feature in both types of models is that they need nucleon pairing in most, if not all, of the core. With fast neutrino cooling nucleon pairing is needed to stop the early cooling which, without this, would produce a star of temperature much lower that the observed one. If the fast neutrino emission is from hyperonic processes it is possible that the suppression we observe is due to hyperon superfluidity. Since fast neutrino emission occurs down to the very center of the core these scenarios need pairing up to the highest density reached in this object. With the slow cooling model ('standard model') superfluidity is also needed, but for a different reason. The observed temperature is below what the simple model predicts, but since this star is cooling by photon emission we can accelerate the cooling at this time by decreasing the specific heat through pairing. If we accept an age of 3×10^5 years and a temperature of 5×10^5 K then the specific heat must have been reduced to about 25% of its normal value. This can be obtained either by pairing of the neutrons in the whole core or by a combination of both neutron and proton pairing, but even in this case most of the neutrons must be paired. If both neutrons and protons are paired in the whole core then a substantial amount of reheating is needed, but several possible mechanisms have been proposed and they can provide sufficient reheating.

As a final point it should be mentioned that this results will have important consequences in modeling the cooling of other neutron stars. For example the cooling calculations of [34] indicate that the Vela pulsar and PSR0656+14 have temperature slightly lower than what the standard model predicts without superfluidity: including some pairing in agreement with the present analysis will raise the theoretical prediction and make the discrepancy larger, reinforcing the case for the occurence of fast cooling in these two objects.

Acknowledgments

I am gratefull to T. Ainsworth, J. H. Applegate, J. P. Halpern, M. Prakash and M. Ruderman for discussions. This work was supported by a HEA-NASA grant NAGW 3075 and a fellowship from the Swiss National Science Fundation.

References

[1] Bignami G F, Caraveo P A and Lamb R C 1983 *Ap. J. Lett.* **272** L9–13

[2] Fichtel C E et al. 1975 *Ap. J.* **198** 163–182

[3] Swanenburg B N et al. 1981 *Ap. J. Lett.* **243** L69-73

[4] Bignami G F, Caraveo P A and Paul J L 1988 *Astron. & Astrophys.* **202** L1-4

[5] Halpern J P and Tytler D 1988 *Ap. J.* **330** 201–217

[6] Halpern J P and Holt S S 1992 *Nature* **357** 222–224

[7] Bertsch D L et al. 1992 *Nature* **357** 306–307

[8] Bignami G F and Caraveo P A 1992 *Nature* **357** 287

[9] IAU circ. # 5649

[10] Michel F C 1991 *Theory of Neutron Star Magnetospheres* (Chicago: The University of Chicago Press)

[11] Lyne A G and Graham-Smith F 1990 *Pulsar Astronomy* (Cambridge: Cambridge University Press)

[12] Lyne A G, Anderson B and Salter M J 1982 *M.N.R.A.S.* **2201** 503–520

[13] Halpern J P and Ruderman M 1992 Submitted to *Ap. J.*

[14] Romani R 1987 *Ap. J.* **313** 718–726

[15] Miller M C 1992 *M.N.R.A.S.* **255** 129–145

[16] Shibanov Y A, Zavlin V E, Palvov G G and Ventura J 1992 To be published in *Astron. & Astrophys.*

[17] Gudmundsson E H, Pethick C J and Epstein R I 1982 *Ap. J. Lett.* **259** L19–23

[18] Pethick C J 1992 *Rev. Mod. Phys.* 64 1133–40

[19] Prakash M, Prakash M, Lattimer J and Pethick C J 1992 *Ap. J. Lett.* **390** L77–80

[20] Friman B L and Maxwell O V 1979 *Ap. J.* **232** 541–557

[21] Brown G E, Kubodera K, Page D and Pizzochero P 1988 *Phys. Rev.* **D37** 2042–46

[22] Maxwell O, Brown G E, Campbell D K, Dashen R F and Manassah J T 1977 *Ap. J.* **216** 77–85

[23] Lattimer J M, Pethick C J, Prakash M and Haensel P 1991 *Phys. Rev. Lett.* **66** 2701–04

[24] Iwamoto N 1980 *Phys. Rev. Lett.* **44** 1637–40

[25] Chao N, Clark J W and Yang C 1972 *Nucl. Phys.* **A179** 320–332

[26] Takatsuka T 1973 *Prog. Theor. Phys.* **50** 1754–55

[27] Niskanen J A and Sauls J A 1981 *Preprint*

[28] Amundsen L and Østgaard E 1985 *Nucl. Phys.* **A437** 487–508

[29] Wambach J, Ainsworth T L and Pines D 1991 *Neutron Stars : Theory and Observation* ed J Ventura and D Pines (Dordrecht: Kluwer Academic Publisher) pp 37–48

[30] Hoffberg M, Glassgold A E, Richardson R W and Ruderman M 1970 *Phys. Rev. Lett.* **24** 775–777

[31] Takatsuka T 1972 *Prog. Theor. Phys.* **48** 1517–33

[32] Jackson A D, Krotscheck E, Meltzer D E and Smith R A 1982 *Nucl. Phys.* **A386** 125–165

[33] Amundsen L and Østgaard E 1985 *Nucl. Phys.* **A442** 163–188

[34] Page D and Applegate J H 1992 *Ap. J. Lett.* **394** L17–20

[35] Bailin D and Love A 1984 *Phys. Rep.* **107** 325–385

[36] Ainsworth T L, Wambach J and Pines D 1989 *Phys. Lett.* **B222** 173–178

[37] Page D and Baron E 1990 *Ap. J. Lett.* **354** L17–20

[38] Friedman B and Pandharipande V R 1981 *Nucl. Phys.* **A361** 502–520

[39] Wiringa R B, Fiks V and Fabrocini A 1988 *Phys. Rev.* **C38** 1010–37

[40] Müther H, Prakash M and Ainsworth T L 1987 *Phys. Lett.* **199B** 469–474

[41] Prakash M, Ainsworth T L and Lattimer J M 1988 *Phys. Rev. Lett.* **61** 2518–21

[42] Nomoto K and Tsuruta S 1987 *Ap. J.* **312** 711–726

[43] Riper K A V 1991 *Ap. J. Suppl.* **75** 449–462

[44] Shibazaki N and Lamb F 1989 *Ap. J.* **346** 808–822

[45] Cheng K S, Chau W Y, Zhang J L and Chau H F 1992 *Ap. J.* **396** 135–146

[46] Hernquist L 1985 *M.N.R.A.S.* **213** 313–336

THE ASTROPHYSICAL JOURNAL, 394: L17–L20, 1992 July 20

THE COOLING OF NEUTRON STARS BY THE DIRECT URCA PROCESS

DANY PAGE AND JAMES H. APPLEGATE
Department of Astronomy, Columbia University, 538 West 120th Street, New York, NY 10027
Received 1992 February 5; accepted 1992 May 1

ABSTRACT

Recent work has shown that many modern nuclear equations of state give proton fractions that are large enough for the direct Urca process to operate in the interiors of neutron stars. We include the direct Urca process in calculations of neutron star cooling and find that the surface temperature of a young neutron star drops catastrophically after $\sim 10^2$ yr if the direct Urca process is allowed and nucleons do not become superfluid. If nucleon superfluidity occurs throughout the direct Urca region, the surface temperature drops to a value determined by the superfluid transition temperature after $\sim 10^2$ yr and decreases slowly for the next $\sim 10^5$ yr, at which time surface photon cooling takes over. The surface temperatures of all of the candidates for thermal X-ray emission from cooling neutron stars are determined by the transition temperature for superfluidity and almost nothing else if these stars cool by direct Urca. By comparison with observational data, we find that superfluid transition temperatures of the order of 10^9 K are required in the whole direct Urca inner core. If neutron stars are created with a range of masses, it is possible that the more massive cool by direct Urca and the less massive do not, resulting in two populations of stars differing in their thermal properties.

Subject headings: dense matter — stars: neutron — X-rays: stars

1. INTRODUCTION

Recent work (Lattimer et al. 1991) has shown that many modern nuclear equations of state have large enough symmetry energies and predict sufficiently high central densities to allow the direct Urca process to operate in the interiors of neutron stars. The neutrino emissivity of the direct Urca process is orders of magnitude larger than that of the modified Urca process and those in all scenarios involving nonnucleonic degrees of freedom (pion condensate, kaon condensate, quark matter, etc.). The Lattimer et al. (1991) result clearly necessitates a complete reexamination of the theory of neutron star cooling. In this *Letter* we report the first results from our program to perform such a reanalysis.

In the absence of nucleon superfluidity, the interior of a star which cools by the direct Urca process cools very rapidly. The surface temperature of such a star drops catastrophically once the crust completes its thermal relaxation, which typically requires $\sim 10^2$ yr. Neutron or proton superfluidity suppresses neutrino emission and halts the rapid cooling because nucleons must be excited above the gap in order to participate in the Urca process. Nucleon superfluidity stabilizes the surface temperature at a value determined by the superfluid transition temperature in the interior and almost nothing else. The qualitative effect of superfluidity shutting off rapid neutrino emission was noted by Page & Baron (1990), who studied the effect of kaon condensation on neutron star cooling.

The thermal histories of stars which cool by direct Urca and those which do not are very different. If neutron stars are created with a range of masses comparable to the mass range of the iron cores of their progenitors, it is possible that the more massive stars cool by direct Urca and the less massive cool by less efficient means. We illustrate the dramatic effect of direct Urca cooling by choosing an equation of state which has a minimum mass of $M_{\rm crit} = 1.35\ M_\odot$ for the onset of direct Urca cooling and presenting cooling curves for stars in the mass range $1.0\ M_\odot < M < 1.7\ M_\odot$. The difference is striking, but the quantitative degree to which neutron stars fall into two thermal populations requires the careful treatment of the role of hyperons and a possible hyperon Urca process (Prakash et al. 1992).

2. THE MODEL

We solve the relativistic equations for heat transport through an unmagnetized neutron star using the Heyney-type stellar evolution code described in detail in Page (1989) and Page & Baron (1990, 1991). We use a nuclear equation of state with a symmetry energy allowing the direct Urca process, and we use the Lattimer et al. (1991) value for the neutrino emissivity due to the direct Urca process. Other than these, the only change is that we use improved calculations of the Coulomb logarithm for electron conductivity in the crust liquid phase by Yakovlev (1987).

The nuclear symmetry energy is the most important factor determining whether or not the direct Urca process is allowed in the star. We parameterize the core equation of state using the functional form suggested by Prakash, Ainsworth, & Lattimer (1988). These authors define the nuclear symmetry energy $S(n)$ by writing the energy per nucelon as

$$E(n, x) = E(n, 0.5) + S(n)(1 - 2x)^2 ,$$

where $x = Z/A$ is the proton fraction, n is the number density of nucleons, and $E(n, 0.5)$ is the energy per nucleon of symmetric nuclear matter. We choose a symmetry energy of $S(n) = 30(n/n_0)^{0.7}$ MeV, where $n_0 = 0.16\ {\rm fm}^{-3}$ is the saturation density of symmetric nuclear matter. This choice is typical of the symmetry energies found in the relativistic equations of state analyzed by Lattimer et al. (1991). We take the other parameters from the second line of Table 1 in Prakash et al. (1988). These parameters give a compression modulus of $K_0 = 180$ MeV, which is the number advocated by conventional wisdom, a maximum neutron star mass of $1.7\ M_\odot$, and a critical mass above which the direct Urca process is allowed of $M_{\rm crit} = 1.35\ M_\odot$.

Superfluidity alters both the specific heat of the superfluid species and the neutrino emissivity because of the gap that it introduces into the excitation spectrum. At low density the pairing is predicted to be in the $^1S_0$ state for both neutrons and protons. At high density the neutron pairing is expected to shift to $^3P_2$ pairing. We treat the suppression of the specific heat following Maxwell (1979). For core neutrino processes (direct Urca, modified Urca, and nucleon bremsstrahlung), we multiply the normal state neutrino emissivity by one Boltzmann factor $\exp(-\Delta/kT)$, where Δ is the relevant gap, for each participating superfluid nucleon.

Neutron $^1S_0$ pairing occurs in the inner crust only. Crust neutron superfluidity has little effect on the cooling of a young neutron star. It may become important if older neutron stars are reheated by the motion of vortices unpinned in pulsar glitches (Alpar et al. 1984), but we do not include this effect in our model. Thus, our calculations will underestimate the surface temperatures of older neutron stars. We take our treatment of $^1S_0$ neutron pairing from Ainsworth, Wambach, & Pines (1989).

Proton $^1S_0$ pairing is the subject of some controversy. Several authors (Chao, Clark, & Yang 1972; Takatsuka 1973; Niskanen & Sauls 1981; Amundsen & Østgaard 1985a) have found that proton superfluidity occurs, but that the $^1S_0$ gap vanishes when the proton Fermi momentum reaches ≈ 1.0–1.2 fm^{-3}. If this result is true, proton $^1S_0$ pairing will have almost no effect on direct Urca cooling because any equation of state which allows the direct Urca process to operate will have proton Fermi momenta much larger than this. A possibly different result is indicated by the work of Wambach, Ainsworth, & Pines (1991). These authors include a treatment of polarization effects and find that the proton $^1S_0$ gap is smaller than that found in previous calculations, but that the gap does not seem to decrease with increasing density. Because of this uncertainty we have performed a calculation using the gap found by Chao et al. (1972), which has almost no effect, and calculations with several density independent transition temperatures, which have a large effect because the superfluidity extends throughout the direct Urca core in the inner part of the star.

Neutron $^3P_2$ pairing has been calculated by Hoffberg et al. (1970), Takatsuka (1972), and Amundsen & Østgaard (1985b). The transition temperatures found in these calculations differ by almost an order of magnitude. In addition, Takatsuka (1972) finds that the gap vanishes at a neutron Fermi momentum of 2 fm^{-1} while the other two calculations find that the gap persists to a much higher density. The chief culprit in the uncertainty seems to be the treatment of dispersion effects. In addition, none of the calculations has included a treatment of polarization effects, and preliminary calculations by Jackson et al. (1982) indicate that they strongly enhance the pairing. We present calculations using the neutron $^3P_2$ gaps found in each of these calculations.

3. RESULTS

3.1. *Observational Data*

There are several promising candidates for the detection of thermal X-rays from cooling neutron stars, but none of them is definitive. We plot the inferred surface temperature or the upper limit on the surface temperature for six of the best candidates on Figures 2 and 3 for comparison with our cooling curves. For Vela (Ögelman & Zimmermann 1989) and PSR 1055−52 (Brinkmann & Ögelman 1987), a blackbody spectrum gave the best fit to the *EXOSAT* data. The *Einstein Observatory* HRI failed to resolve the sources RCW 103 (Tuohy et al. 1983) and PSR 0656+14 (Córdova et al. 1989), suggesting that the observed X-rays were emitted from the surface of the star rather than from a synchrotron nebula surrounding the star. However, *ROSAT* has not detected the compact source in RCW103, giving thus an upper limit of 1.2×10^6 K on its temperature (Becker 1992). The surface temperatures for 3C 58 (Becker, Helfand, & Szymkowiak 1982) and the Crab (Harnden & Seward 1984) are upper limits based on *Einstein* data.

All of the surface temperatures plotted in the figures are the temperature measured by an observer at infinity.

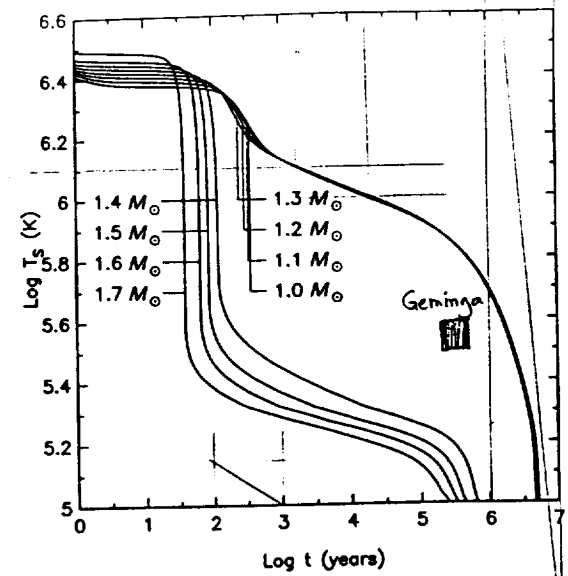

FIG. 1.—Cooling with and without the direct Urca process. The surface temperature at infinity for several star masses and no nucleon superfluidity are shown. Stars with $M > 1.35\ M_\odot$ cool by the direct Urca process; stars with $M < 1.35\ M_\odot$ do not.

3.2. *Cooling without Superfluidity*

The dramatic effect of the direct Urca process on the thermal evolution of a neutron star is demonstrated in Figure 1, which shows the cooling curves for the neutron star models listed in Table 1. Nucleon superfluidity is neglected in all calculations. Our equation of state has a minimum mass of 1.35 $M_\odot$ for the onset of the direct Urca process, so the models with $M \geq 1.4\ M_\odot$ cool by direct Urca and the models with $M \leq 1.3\ M_\odot$ do not. The photon luminosity of a direct Urca star in the age

TABLE 1

PROPERTIES OF NEUTRON STARS OF VARIOUS MASSES

M_{star}	R_{star}	M_{core}	R_{core}	M_{pit}	R_{pit}	ρ_c
1.0	11.910	0.897	9.76	0	0	2.94
1.1	11.780	1.007	9.90	0	0	3.28
1.2	11.630	1.119	9.99	0	0	3.67
1.3	11.460	1.228	10.03	0	0	4.15
1.4	11.250	1.339	10.02	0.038	2.405	4.76
1.5	10.970	1.448	9.93	0.212	4.169	5.58
1.6	10.570	1.560	9.72	0.489	5.345	6.91
1.7	9.470	1.674	8.91	1.003	6.238	12.07

NOTE.—Masses and radii of the stars, their cores, and, for $M > 1.35\ M_\odot$, their inner cores ("pit") where the direct Urca process is allowed. Masses are in solar masses and radii in km. The last column gives the central density in units of nuclear matter density $\rho_0 = 2.8 \times 10^{14}$ g cm^{-3}.

range 10^2–10^5 yr is roughly 10^4 times smaller than a modified Urca star of the same age. Note that the direct Urca process has an enormous effect even if the fraction of the core in which it is allowed is very small (see the 1.4 $M_\odot$ case). The mass dependence of the surface temperature for the direct Urca stars of age 10^2–10^5 yr is due to the more massive stars having larger direct Urca cores.

After a rapid initial cooling phase, which lasts roughly a year, the surface temperature stays on a plateau for several decades. The duration of the plateau phase is determined by the thermal time scale of the crust. The systematic effect of the more massive stars leaving the plateau the earliest is due to the fact that the more massive a neutron star is, the less massive a crust it has. The smaller crusts of the more massive stars have shorter thermal time scales. The level of the plateau is determined by the properties of the crust, so the surface temperature during this phase of the cooling is independent of the cooling rate of the core. The dramatic difference between direct Urca cooling and modified Urca cooling appears once the crust has thermally relaxed and the star leaves the plateau.

3.3. *The Effect of Core Neutron Superfluidity*

Cooling curves for the 1.4 $M_\odot$ neutron star using various results for the $^3P_2$ neutron pairing gap and allowing for the direct Urca process are given in the solid curves in Figure 2. All curves include crust neutron superfluidity with the $^1S_0$ gap calculated by Ainsworth et al. (1989) and proton superfluidity with the $^1S_0$ gap calculated by Takatsuka (1972), but neither of these gaps has any significant effect on the cooling. For comparison, the dashed curve has no $^3P_2$ neutron pairing and the two dotted curves correspond to a 1.3 $M_\odot$ star cooling without direct Urca, with and without $^3P_2$ neutron pairing.

The qualitative effect of core neutron superfluidity is to halt the rapid cooling of the interior once the interior has reached the superfluid transition temperature. This results in higher surface temperatures once the crust has completed its thermal relaxation. Roughly speaking, the surface temperature stabilizes at $T_s = T_s(\alpha T_c)$, where T_c is the superfluid critical temperature, α is typically $\simeq 0.2$, and $T_s(T_{\rm int})$ is the surface temperature–interior temperature relation found by Gudmundsson, Pethick, & Epstein (1982, 1983) and Hernquist & Applegate (1984).

This qualitative picture is borne out by the detailed calculations presented in Figure 2. The cooling curves labeled HGRR, 0.3HGRR, and 0.1HGRR have the neutron $^3P_2$ gap calculated by Hoffberg et al. (1972), and that gap multiplied by 0.3 and 0.1. The curve labeled AO uses the gap calculated by Amundsen & Østgaard (1985b), and the curve labeled T72 uses the calculation of Takatsuka (1972). Core neutron superfluidity with the Takatsuka (1972) gap has almost no effect on the cooling because the gap vanishes in the direct Urca core of our star; there is no superfluidity where it is needed. For the rest of the models, the larger gaps give higher surface temperatures. Multiplying the Hoffberg et al. (1972) gap by 0.1 lowers the cooling curve by just about 0.5 in the log. The $T_s(T_{\rm int})$ relation is $T_s \propto T_{\rm int}^{0.55}$, so the detailed result is exactly what the qualitative picture predicted.

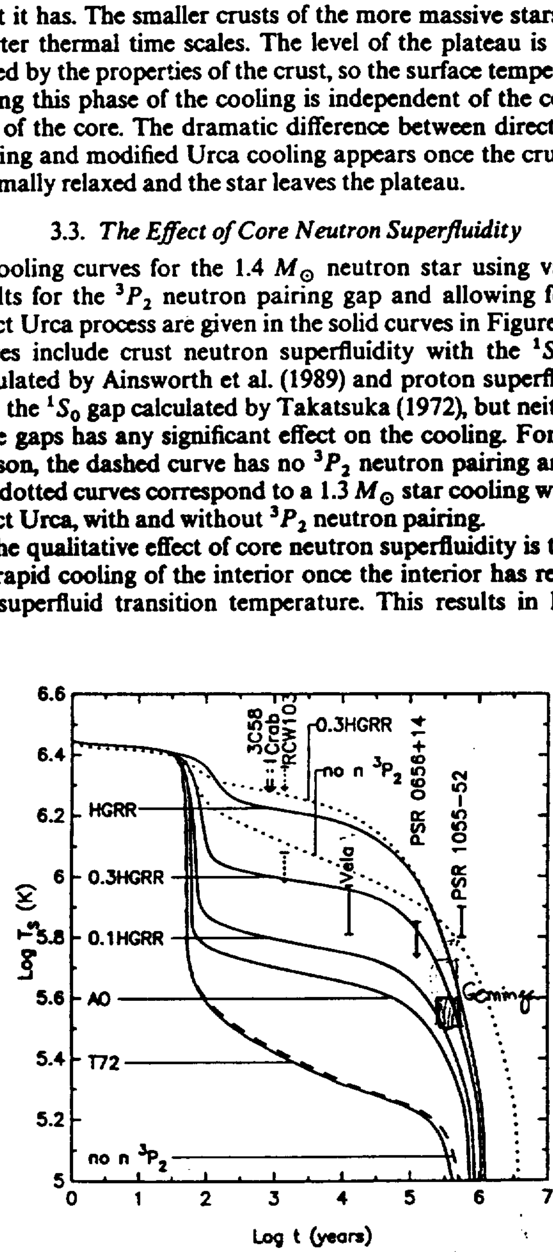

FIG. 2.—Effect of neutron superfluidity on the direct Urca cooling. Cooling curves for a 1.4 $M_\odot$ direct Urca star using various calculations of the neutron $^3P_2$ gap are shown in the solid curves. The labels are defined in the text. The dashed curve has no neutron $^3P_2$ superfluidity. The dotted curves show the cooling of a 1.3 $M_\odot$ star without direct Urca, with and without neutron $^3P_2$ pairing for comparison. The sources of the plotted data are given in the text.

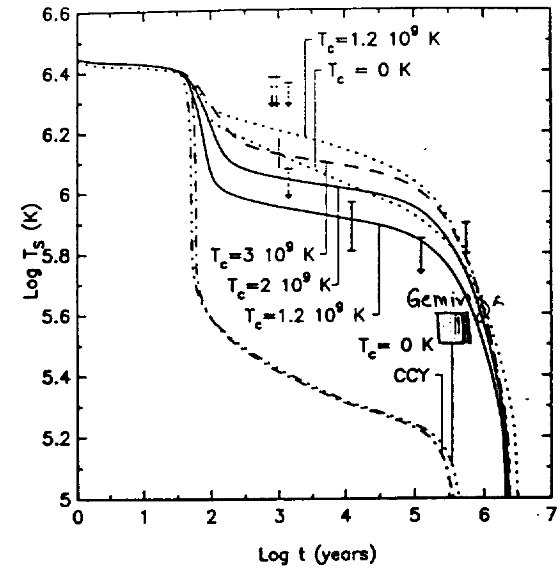

FIG. 3.—Effect of proton superfluidity on direct Urca cooling. Cooling curves for a 1.4 $M_\odot$ direct Urca star using various assumptions about the proton $^1S_0$ gap are shown. The dash-dot curve uses the proton gap found by Chao et al. (1972). The dashed curve and the two solid curves have been computed using density-independent critical temperature for proton $^1S_0$ superfluidity as labeled. The dotted curves show the cooling of a 1.3 $M_\odot$ star without direct Urca, with and without proton pairing for comparison.

3.4. *The Effect of Proton Superfluidity*

The effect of proton superfluidity on the cooling of the 1.4 $M_\odot$ star is illustrated in Figure 3. All curves have been calculated using the $^1S_0$ neutron gap of Ainsworth et al. (1989) and the $^3P_2$ neutron gap of Takatsuka (1972). Neither of these neutron gaps affects the cooling significantly. The dot-dash curve (CCY) has been calculated using the proton gap obtained by Chao et al. (1972). This proton gap vanishes in the inner core in which the direct Urca process is allowed in this model, so proton superfluidity has almost no effect on the cooling, as can be seen by comparing with the triple dot-dash curve which has no proton superfluidity at all. The two dotted curves are for comparison purposes. They correspond to a 1.3 $M_\odot$ star, which cools without direct Urca, with and without proton superfluidity. The two solid curves give results of calculations in which density-independent critical temperatures of 1.2 and 2×10^9 K for proton superfluidity have been used, corresponding to the upper and lower values found by Wambach et al. (1991), and the dashed one has a higher critical temperature of 3×10^9 K. These curves show a large effect due to proton superfluidity because the superfluidity, by assumption, occurs throughout the direct Urca core in the center of the star. The one with $T_c = 3 \times 10^9$ K gives temperatures even larger than the models with only modified Urca processes and no superfluidity.

4. CONCLUSIONS

We have included the direct Urca process in calculations of the cooling of young neutron stars and found that stars in which the direct Urca process is allowed cool to invisibility as soon as the thermal relaxation of the crust has been completed unless nucleon superfluidity intervenes. This qualitative result is independent of the size of the inner core in which the direct Urca process occurs; direct Urca cooling is so efficient it dominates the cooling if it is allowed anywhere in the star. Superfluidity of either neutrons or protons can shut off the direct Urca process and halt the drop of the surface temperature, but the entire direct Urca inner core must become superfluid. If superfluidity occurs and shuts off the direct Urca process, the surface temperature of the star stays essentially constant until the star is $\gtrsim 10^5$ yr old, at which time surface photon cooling takes over and the cooling speeds up. *Direct Urca stars in the age range* 10^2–10^5 *yr old are thermometers for nucleon superfluidity* because their surface temperatures are determined by the superfluid transition temperature in the direct Urca inner core and almost nothing else.

Figures 2 and 3 show that the Vela pulsar and PSR 0656+14 have surface temperature below the standard cooling curves, as already found by Nomoto & Tsuruta (1986, 1987) and Page & Baron (1990, 1991), and thus require some enhanced cooling controlled by nucleon superfluidity. *Superfluidity transition temperatures of the order of* 10^9 K *are then required down to the center of the star*, if the reported temperatures of these two objects are indeed surface temperatures. Drawing a more quantitative conclusion will require the inclusion of nucleon isobars and hyperon processes and a more accurate treatment of the effect of $^3P_2$ pairing on the neutrino emissivity, as well as better data. Older stars (e.g., PSR 1055−52) may have significant heating from the motion of the superfluid vortex lines in their crusts.

The nuclear symmetry energy is the most important factor in determining whether or not the direct Urca process is allowed in neutron stars. Our results have been obtained with an equation of state whose symmetry energy was adjusted to give the onset of direct Urca cooling at 1.35 $M_\odot$. While this choice was made to illustrate the dramatic effect that direct Urca cooling can have, we do not believe that this choice seriously limits the significance of our results. Our neutron star models, summarized in Table 1, have quite standard radii and central densities. Our equation of state has a standard value for the compression modulus of symmetric nuclear matter, and our symmetry energy is consistent with that found by Lattimer et al. (1991) for relativistic nuclear equations of state. We conclude, in agreement with Lattimer et al. (1991), that direct Urca cooling in neutron stars is consistent with all constraints on the nuclear equation of state, and its possible occurrence must be considered in neutron star cooling calculations.

Neutron stars are probably born with a range of masses. If the range of iron core masses of their progenitors translates into a similar range of neutron star masses, then a mass range of 0.2–0.4 $M_\odot$ is expected. It is possible that the more massive stars cool by direct Urca and the less massive stars do not. In this case neutron stars will divide into two populations, differing substantially in their thermal histories.

We thank T. L. Ainsworth, L. Bildstein, M. Prakash, & D. G. Yakovlev for suggestions and discussions and an anonymous referee for his suggestions. Many of these calculations were performed on the Vax cluster of the Nuclear Theory Group at SUNY, Stony Brook. This work has been supported by a grant from NASA. One of us (D. P.) acknowledges support from the Swiss National Science Foundation.

REFERENCES

Ainsworth, T. L., Wambach, J., and Pines, D. 1989, Phys. Lett., B222, 173
Alpar, M. A., Anderson, P. W., Pines, D., & Shaham, J. 1984, ApJ, 276, 325
Amundsen, L., & Østgaard, E. 1985a, Nucl. Phys. A, 437, 487
———. 1985b, Nucl. Phys. A, 442, 163
Becker, R. H., Helfand, D. J., & Szymkowiak, A. E. 1982, ApJ, 255, 557
Becker, W. 1992, private communication and poster presented at the meeting Physics of Isolated Pulars, Taos (New Mexico)
Brinkmann, W., & Ögelman, H. 1987, A&A, 182, 71
Chao, N.-C., Clark, J. W., & Yang, C.-H. 1972, Nucl. Phys. A, 179, 320
Córdova, F. A., Hjellming, R. M., Mason, K. O., & Middleditch, J. 1989, ApJ, 345, 451
Gudmundsson, E. H., Pethick, C. J., & Epstein, R. 1982, ApJ, 259, L19
———. 1983, ApJ, 272, 286
Harnden, F. R., Jr., & Seward, F. D. 1984, ApJ, 283, 279
Hernquist, L., & Applegate, J. H. 1984, ApJ, 287, 244
Hoffberg, M., Glassgold, A. E., Richardson, R. W., & Ruderman, M. 1970, Phys. Rev. Lett., 24, 775
Jackson, A. D., Krotscheck, E., Meltzer, D. E., & Smith, R. A. 1982, Nucl. Phys. A, 386, 125
Lattimer, J. M., Pethick, C. J., Prakash, M., & Haensel, P. 1991, Phys. Rev. Lett., 66, 2701
Maxwell, O. V. 1979, ApJ, 231, 201
Niskanen, J. A., & Sauls, J. A. 1981, unpublished
Nomoto, K., & Tsuruta, S. 1986, ApJ, 305, L19
———. 1987, ApJ, 312, 711
Ögelman, H., & Zimmermann, H.-U. 1989, A&A, 214, 179
Page, D. 1989, Ph.D. thesis, SUNY at Stony Brook
Page, D., & Baron, E. 1990, ApJ, 354, L17
———. 1991, ApJ, 382, L111
Prakash, M., Ainsworth, T. L., & Lattimer, J. M. 1988, Phys. Rev. Lett., 61, 2518
Prakash, M., Prakash, M., Lattimer, J., & Pethick, C. J. 1992, ApJ, 390, L77
Takatsuka, T. 1972, Prog. Theor. Phys., 48, 1517
———. 1973, Prog. Theor. Phys., 50, 1754
Tuohy, I. R., Garmire, G. P., Manchester, R. N., & Dopita, M. A. 1983, ApJ, 268, 778
Wambach, J., Ainsworth, T. L., & Pines, D. 1991, in Neutron Stars: Theory and Observation (Proceedings of the NATO Advanced Study Institute, Agia Pelagia, Crete, Greece), ed. J. Ventura & D. Pines (Dordrecht: Kluwer), 37
Yakovlev, D. G. 1987, Soviet Astr., 31, 347